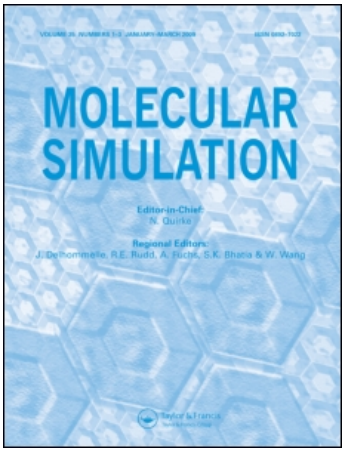

Molecular Simulation
Publication details, including instructions for authors and subscription information:
http://www.informaworld.com/smpp/title~content=t713644482

Molecular Dynamics Studies of Diffusion in Model Cylindrical Pores at Very Low Densities

George K. Papadopoulos[a]; David Nicholson[a]; Soong-Hyuck Suh[b]
[a] Computational and Structural Group, Department of Chemistry, Imperial College of Science Technology and Medicine, London [b] Department of Chemical Engineering, Keimyung University, Taegu, Korea

To cite this Article Papadopoulos, George K. , Nicholson, David and Suh, Soong-Hyuck(1999) 'Molecular Dynamics Studies of Diffusion in Model Cylindrical Pores at Very Low Densities', Molecular Simulation, 22: 4, 237 — 256
To link to this Article: DOI: 10.1080/08927029908022099
URL: http://dx.doi.org/10.1080/08927029908022099

Molecular Simulation, 1999, Vol. 22, pp. 237–256
Reprints available directly from the publisher
Photocopying permitted by license only

MOLECULAR DYNAMICS STUDIES OF DIFFUSION IN MODEL CYLINDRICAL PORES AT VERY LOW DENSITIES

GEORGE K. PAPADOPOULOS[a], DAVID NICHOLSON[a,*] and SOONG-HYUCK SUH[b]

[a] *Computational and Structural Group, Department of Chemistry, Imperial College of Science Technology and Medicine, London SW7 2AY;*
[b] *Department of Chemical Engineering, Keimyung University, Taegu 704-701, Korea*

(Received December 1998; accepted December 1998)

Molecular dynamics simulation has been used to study diffusion of methane at ambient temperature in cylindrical pores at very low densities. The cylinders were modelled as a continuum solid which interacts with the methane in the radial direction only. At the lowest densities, the VACF method does not yield reliable values of the self diffusion coefficient, D_s, but a suitable choice of time step and run length enables values of D_s to be found from MSD plots that are below the classical Knudsen diffusion coefficients. When density is increased, D_s passes through a maximum although the adsorption isotherm remains inside the Henry law region. Maxima are found for two cylinder radii and for two adsorbent field strengths. The existence of a maximum is attributed to transient intermolecular interactions. Analysis of a molecular trajectory demonstrates that long diffusion paths can be triggered by the rare event of an intermolecular encounter which forces a molecule into the repulsive part of the wall potential. At sufficiently high density, subsequent collisions quench the tendency towards long paths, and D_s decreases again. The issue of simulation artefact as a source of these observations is discussed.

Keywords: Diffusion; methane; cylindrical pores

1. INTRODUCTION

Molecular dynamics has been used widely in recent years for the computation of the positions and conjugate momenta of microscopic model systems, through numerical integration of the equations of motion.

*Corresponding author.

Application of this technique in the area of the transport phenomena through porous media, in conjunction with the linear response theory [1–4], offers a useful tool in the study of the transport coefficients. This is especially so since interpretation of the experimental measurements of this kind in microporous media, is often controversial [3].

Both equilibrium and non-equilibrium molecular dynamics studies have been used to investigate self and transport diffusion coefficient values over a range of adsorbate loadings for various hydrocarbons and inorganic molecules in carbonaceous micropores and zeolites, as well as in idealised pore models [5–14]. Previous work in this laboratory on the transport properties of methane in a graphite slit-shaped pore at ambient temperatures using equilibrium isothermal (NVT) molecular dynamics, has demonstrated the dependence of the self-diffusion coefficient D_s for different pore sizes, on the concentration of the adsorbed phase [12–14]. One of the observations of that work, was the prediction of an initial increase of the self-diffusion coefficient close to the lower concentration limit (Henry's law region). Similar results had previously been observed in zeolites [7, 10]. In both of these studies, the field of the zeolite was represented by a complicated potential surface and the enhanced initial diffusivity was attributed to molecular collisions which caused molecules trapped in local potential minima to escape and contribute to the total flux. However, the same phenomenon was observed in slit pores [12–14] where the potential was energetically homogeneous in directions parallel to the surface.

In a theoretical study of free molecule flux through model pores [15], molecular trajectories were found using Monte Carlo methods and used to calculate fluxes by statistical weighting. It was shown that the adsorbent field, modelled as an energetically continuum solid, can affect the molecular trajectories at the zero concentration limit. Trajectories in slit pores for example, can be subdivided into two groups depending upon the velocity of a molecule normal to the wall. If the molecule leaving a pore wall exceeds the escape velocity, then it will cross the slit with a trajectory that is longer than the classical linear Knudsen trajectory. On the other hand the trajectories of molecules with less than the escape velocity will pass through a maximum before falling back to the wall. The overall effect is that the flux falls below the Knudsen limit as the strength of the adsorbent field increases (or the temperature decreases), but eventually exceeds the flux for the Knudsen limit at high field strength due to the high concentration of molecules close to the surface. A limitation of these early calculations was that the method requires the assumption of a collision free system at all field strengths. Clearly, as the adsorbent field becomes stronger, this assumption

becomes increasingly suspect. Molecular dynamics removes this limitation, since all molecular interactions, including those between the moving particles can be included.

In none of the previous molecular dynamics studies of diffusion at low loading was it possible to characterise unambiguously the zero coverage Knudsen limit, since this cannot be simply defined in slit pores or in complicated geometries [12, 16]. However in cylindrical geometry this limit is well known. In this work we study diffusion coefficients at very low concentrations by carrying out molecular dynamics in cylindrical pore models with different energetic characteristics for the potential field. The main conclusion from these studies is that, for micropore systems, even when the adsorbate concentration is well inside the Henry's law region, there is a concentration region where molecular trajectories are much larger than those predicted from classical molecular streaming theory. Although large-scale applications of transport in micropore systems often operate at intermediate adsorbate loading, this large increase in the diffusivity is nevertheless of significant theoretical and practical interest. It is often assumed that the longest trajectories in such a system are given by the Knudsen equation and the Knudsen diffusion coefficient is considered to be an ideal upper limit at zero concentration. It should be mentioned that at very low loadings, collective diffusion and viscous contributions to flux tend to zero, and that the Darken correction factor [3] tends to unity, therefore the self diffusion coefficient in this limit is identical to the transport diffusion coefficient.

A crucial point, that emerges from this work, is that the molecular dynamics study of such a dilute system requires the execution of unusually long runs compared to the rest of the density region for this pore geometry. Even on the vector supercomputer used in this work, (a fourteen processor Silicon Graphics Challenge), it requires hundreds of CPU hours to simulate a nanosecond of actual motion with molecular dynamics. This makes the study of very low concentrations an extremely time consuming procedure. Even so the calculated diffusion coefficients are subject to significant error at the lowest concentration used here. Recently Chitra and Yashonath [17] carried out NVE molecular dynamics runs for low adsorbate concentrations in zeolite NaCaA. They found that their system required an extremely long simulation time (up to 120 ns) in order to get accurate diffusion coefficients. Since the very complicated adsorbent field in their system may be partly responsible for the need for such long computing times, the first part of this work has concentrated on the investigation of the optimum conditions under which the self-diffusion coefficient can be calculated.

2. MODEL DESCRIPTION

The system chosen for study was methane in smooth walled cylindrical pores. The methane molecule was modelled as a single centre Lennard-Jones sphere, with interactions expressed *via* the 12–6 potential with the parameters $\varepsilon_{gg}/k = 148\,\text{K}$ and $\sigma_{gg} = 0.3812\,\text{nm}$. The cross parameters between methane and the solid atoms, were calculated from the Lorentz-Bertholet rules.

The adsorbent surface was represented by a pseudo atom model [18]. In this model, the pores are constructed from close packed layers of simple atoms, whose Lennard-Jones interaction parameters ε_{ss} and σ_{ss} can be varied. The interaction of an adsorbate probe was calculated along a radius in a cross section passing through the centres of a ring of adsorbate atoms, by summation over all the atoms in the cylinder for each probe atom position. In order to generate an energetically smooth walled pore, the potential variation normal to the wall was taken to be the same at any axial position of the cross section.

To estimate the parameters, the model was calibrated against a real system, so that the potential fields of the two systems have comparable adsorption energies for a give adsorbate probe. In the present case, the cylindrical pore model was calibrated against zeolite VPI5 chosen for its similarity to a set of unconnected cylinders with the crystallographic (internal) radius $R' = 0.605\,\text{nm}$ [19]. For the calibration we used the experimental isosteric heat of adsorption at zero coverage for Ar at 77 K [$q_{st}(0) = 10.24\,\text{kJ mol}^{-1}$ $(15.99\,kT)$]. The model surface was considered to consist only of oxide atoms according to the assumption of Kiselev *et al.* [20]. The physical radius of the model pore (*i.e.*, half the distance between adsorbent atom centres across a pore diameter) was calculated to be $R = 0.727\,\text{nm}$ from the relation

$$R = R' + z_0 - \sigma_{ArAr}/2 \tag{1}$$

where $z_0 = 0.8506\,\sigma_{ArO}$ is the distance at which the Ar-oxide plane wall potential passes through zero, $\sigma_{ArAr} = 0.3405\,\text{nm}$.

The theoretical heat of adsorption per molecule at zero adsorbate occupancy is given by the equation

$$q_{st}(0) = kT - \frac{\int_V u(\boldsymbol{r})\mathrm{e}^{-u(\boldsymbol{r})/kT}d\boldsymbol{r}}{\int_V \mathrm{e}^{-u(\boldsymbol{r})/kT}d\boldsymbol{r}} \tag{2}$$

where the last term is the average potential energy $\langle u(\boldsymbol{r})\rangle$ of an isolated methane molecule over the field of the pore volume V.

A reasonable value of $\sigma_{ss} = 0.270\,\text{nm}$ was selected for the hard sphere diameter of oxygen and a physical pore radius of $R = 0.729\,\text{nm}$. Monte Carlo integration of Eq. (2) then gave $q_{st}(0) = 15.96\,kT$ for Ar at 77 K, in a single layer cylinder of oxide atoms. With $\varepsilon_{ss}/k = 395\,\text{K}$ in close agreement to the experimental heat of adsorption for VPI-5. Our basic adsorbent model, with the above parameters, can therefore be regarded as a first approximation to a cylindrical oxide pore.

In some runs, the potential field exerted by the model pore was varied by changing the potential well ε_{ss} of the pseudo-atom interaction. The effect of the pore field on the adsorption energy of methane is shown in the Figure 1.

Since the adsorbent is modelled as a continuum, it is necessary to model the condition for reflection at the wall. In these simulations we used the diffuse reflection model adopted in earlier work [12–14] in which the velocity components parallel to the wall are randomised when the velocity component normal to the wall is reversed inside the minimum of the molecule wall potential energy.

The choice of cylindrical geometry means that the diffusion coefficient at the zero density limit can be compared with that calculated from the

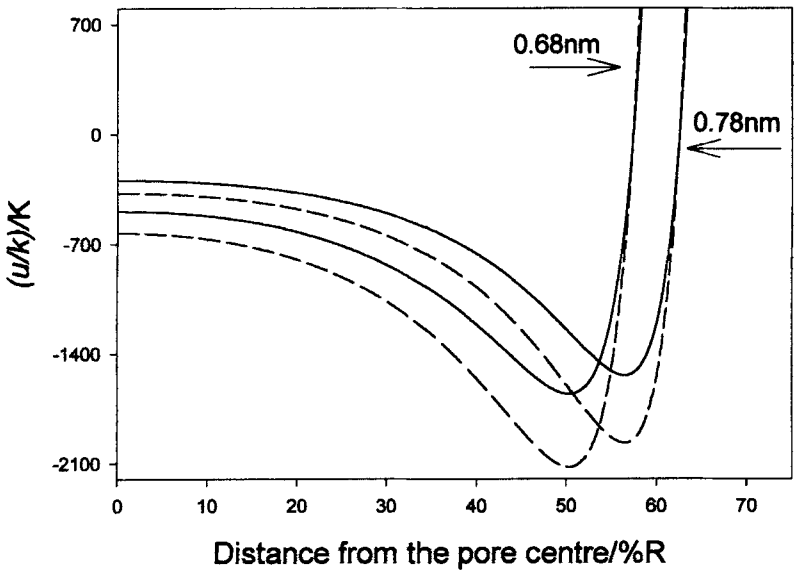

FIGURE 1 Methane-pseudo-atom potential for the cylindrical pore model with $\varepsilon_{ss}/k = 395\,\text{K}$ (solid line) and $\varepsilon_{ss}/k = 650\,\text{K}$ (dashed line).

Knudsen diffusion coefficient value D_k, given by the relation:

$$D_k = \frac{2}{3} R_K \bar{v} = \frac{4}{3} R_K \left(\frac{2kT}{\pi m} \right)^{\frac{1}{2}} \tag{3}$$

where $\bar{v}$ is the mean molecular velocity of the molecules having mass m, T is the temperature of the system, and R_K is the effective cylinder radius for Knudsen flow. The latter is the furthest distance from the cylinder centre that a molecule centre can travel. Clearly, this quantity cannot be precisely defined for soft repulsive potentials. It is therefore assumed that R_K is limited by the hard sphere separation between the wall particles and the adsorbate *i.e.*,

$$R_K = R - \sigma_{gs} \tag{4}$$

In the usual reduced MD units [21], Eq. (3) becomes:

$$D_k^* = \frac{4}{3} R_K^* \left(\frac{2T^*}{\pi} \right)^{\frac{1}{2}} \tag{5}$$

3. RESULTS

3.1. Methodology

The concentration of methane in the pore was calculated by generating the adsorption isotherm using the grand canonical Monte Carlo technique [21]. The self-diffusion coefficient has been calculated using both integration of the velocity auto-correlation function (VACF) and the time-evolution of the mean squared displacement method (MSD) [21].

Two physical pore sizes were used in the calculations: $R = 0.68$ nm and $R = 0.78$ nm. Using Eqs. (4) and (5) the corresponding reduced Knudsen radii (R_K^*) are 0.930 and 1.192, and the reduced Knudsen diffusion coefficients are 1.40 and 1.79 respectively. The adsorption and self-diffusivity of methane at 298 K, was calculated for reduced number densities $\rho\sigma^3$ lying in the region from 10^{-5} to 10^{-2}. The results are summarised in Tables I and II. The influence of the field on the molecular distribution of the adsorbate in the radial direction for different values of densities in the pore is shown in Figure 2 and the isotherms, obtained from GCMC simulation, in Figure 3. The latter confirm that the densities studied are well inside the Henry's law region.

TABLE I Molecular dynamics parameters and self-diffusion coefficients D_s^* in reduced units ($D_s m^{1/2}\varepsilon^{-1/2}\sigma^{-1}$) obtained for the model cylindrical pore of radius $R = 0.68$ nm

$\rho\sigma_{gg}^3$	t/ns	$\delta t/fs$	t_c/ns	$D_{s\,MSD}^*$	$D_{s\,VACF}^*$
$2.67 \cdot 10^{-5}$	0.5	1	0.010	0.56	–
	1	1	0.300	0.68	–
	1	2	0.300	1.55[a], 1.39[b]	–
	2	2	0.300	1.58[a], 1.37[b]	–
	5	1	0.005	0.54	–
	5	1	0.300	0.57	–
$2.28 \cdot 10^{-4}$	1	0.5	0.175	3.56	3.11
	1	1	0.300	3.48	3.00
	1	2	0.300	4.17	3.70
	1	3	0.300	1.49[a], 1.25[b]	3.28
$5.34 \cdot 10^{-4}$	1	1	0.020	3.58	3.84
	1	1	0.300	3.50	3.62
	1	2	0.300	3.64	3.75
$1.30 \cdot 10^{-3}$	1	1	0.020	2.58	2.62
	1	1	0.300	2.51	2.48
	1	2	0.020	2.73	2.77
$8.10 \cdot 10^{-2}$	1	1	0.300	0.90	0.94
	1	2	0.030	0.86	0.80

[a] Value of D_s^* calculated from the first slope of the MSD plot.
[b] Value of D_s^* calculated from the second slope of the MSD plot.

TABLE II Molecular dynamics parameters and self-diffusion coefficients D_s^* in reduced units ($D_s m^{1/2}\varepsilon^{-1/2}\sigma^{-1}$) obtained for the model cylindrical pore of radius $R = 0.78$ nm

$\rho\sigma_{CH_4}^3$	t/ns	$\delta t/fs$	t_c/ns	$D_{s\,MSD}^*$	$D_{s\,VACF}^*$
$9.04 \cdot 10^{-6}$	1	1	0.040	0.30	–
	1	1	0.100	0.37	–
	1	2	0.100	0.76	–
$9.04 \cdot 10^{-5}$	0.5	1	0.020	3.17	3.02
	0.5	2	0.100	3.37	3.30
	1	1	0.100	3.23	3.31
$9.00 \cdot 10^{-4}$	0.5	1	0.040	3.46	3.81
	0.5	2	0.040	3.20	3.19
$9.12 \cdot 10^{-3}$	0.5	1	0.040	2.26	2.41
	0.5	2	0.040	2.89	2.86

It may be observed from Table I, that the self-diffusion coefficients are highly dependent on the specified molecular dynamics parameters. Thus D_s varies significantly with the time step δt, for runs of the same total time t, when the time step δt is changed. This behaviour is most noticeable at the very lowest concentrations, and progressively disappears as the concentration increases.

It is expected from earlier work [15] that in the zero concentration limit, D_s^* will be less than or equal to D_K^* when an adsorbent force field is present,

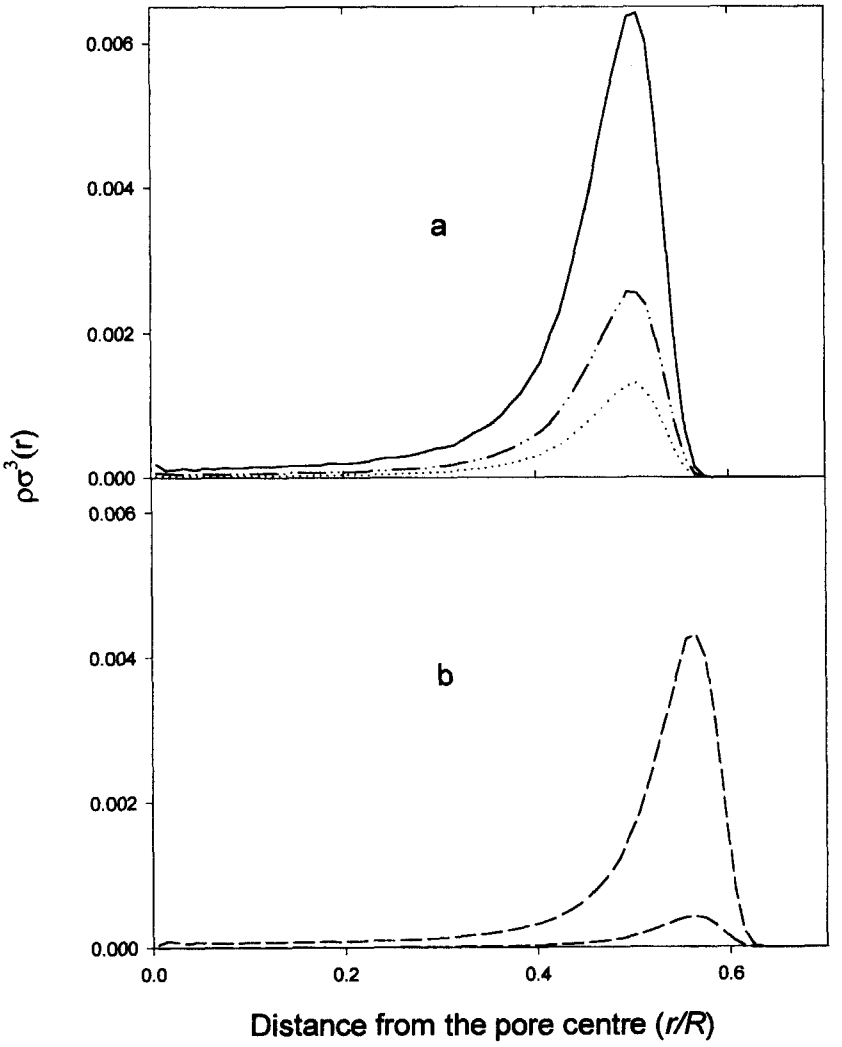

FIGURE 2 Number density $\rho^*(=\rho\sigma^3)$ profiles along the pore radius for (a) $R = 0.68$ nm; at mean densities of $1.30 \cdot 10^{-3}$ (solid line), $5.34 \cdot 10^{-4}$ (dash-dotted line) and $2.67 \cdot 10^{-5}$ (dotted line); (b) $R = 0.78$ nm at mean densities $9.00 \cdot 10^{-4}$ (upper line), $9.04 \cdot 10^{-5}$ (lower line).

since the overall effect is to shorten the molecular trajectories in comparison to the linear Knudsen trajectories. The present investigation suggests that small δt values, rather than long runs, lead to values of D_s^* that meet this criterion. For example when $R = 0.68$ nm (Tab. I) it is seen that, at the lowest concentration studied, the longest run of 5 ns, using the lower values

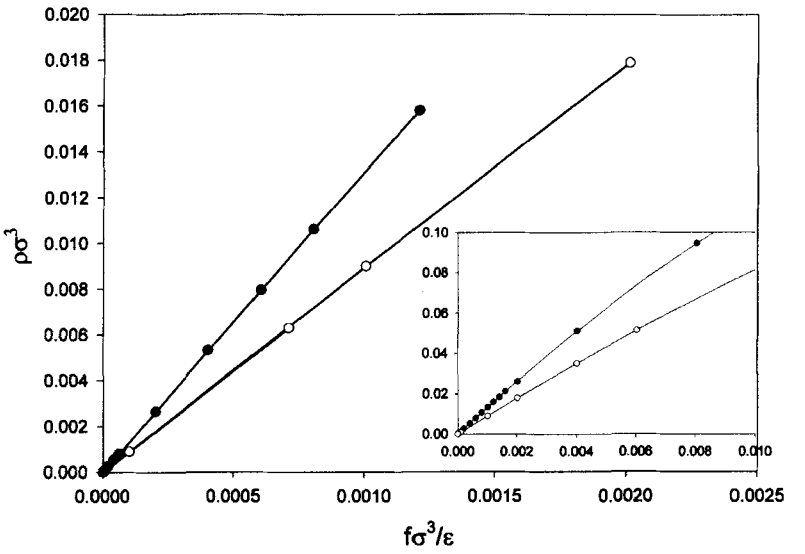

FIGURE 3 Henry law region isotherms for CH_4 at 298 K presented as number density *vs.* reduced fugacity for cylindrical pores of radius 0.68 nm (filled circles) and 0.78 nm (open circles); the inset shows the extension of these isotherms to higher fugacities.

of δt (1 fs) gave $D_s^* = 0.57$ compared with 0.68 for the run lasting 1 ns. In both cases the correlation time t_c in the MSD analysis was 0.300 ns.

It was noted that the smaller time step, gave MSD plots with a linear part at much earlier times. At the lowest concentration in Table I for example, the higher δt value with a run length of 1 ns, gave MSD-plots with two linear sections as illustrated in Figure 4 (top panel), and tend to overestimate D_s at the lowest concentration (giving a value above the classical Knudsen estimate). Due to the method of averaging [14], the final section of the plot suffers from poor statistics since few time origins are included, and has therefore been omitted from the estimate of D_s.

In order to confirm the origin of the second linear part of the MSD curve, we repeated the run at $\rho^* = 2.28 \times 10^{-4}$, increasing the run length from 2 ns to diminish any problem arising from poor statistics. Figure 4 (bottom panel) shows the two runs for 2 fs and 3 fs. The longest time step (Fig. 4d) again produces an MSD plot with a second linear part as observed at the lower concentration. Chitra and Yashonath [17], have likewise observed the advent of a second linear part of the MSD-plot with lower slope above a certain value of t_c. The present calculations suggest that smaller time steps, rather than an increased number of time origins (longer runs), help to minimise this problem. Furthermore, the present investigation shows, that

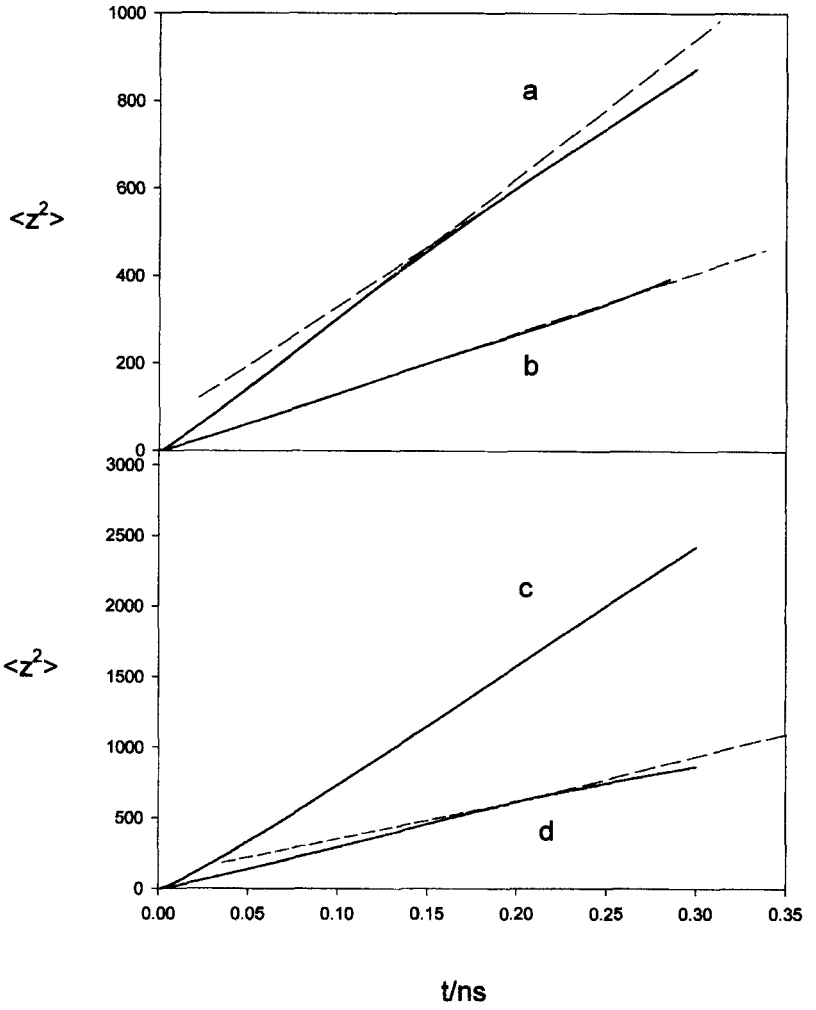

FIGURE 4 Mean square displacement plots along the direction of the flow (z-axis), for R = 0.68 nm and for (a) $\rho^* = 2.67 \cdot 10^{-5}$, $\delta t = 2$ fs; (b) $\rho^* = 2.67 \cdot 10^{-5}$, $\delta t = 1$ fs; (c) $\rho^* = 2.28 \cdot 10^{-4}$, $\delta t = 3$ fs; (d) $\rho^* = 2.28 \cdot 10^{-4}$, $\delta t = 2$ fs.

with suitable choice of δt, a satisfactory estimate of D_s can be obtained without having to use a long correlation time, a procedure which demands large resources. It seems probable that this difficulty arises in these simulations because, close to the wall, molecules are subjected to rapidly varying force fields, which necessitates rather small time steps for accurate calculation. At low concentration trajectories are not randomised through collisions with other molecules, and therefore long trajectories occur

between collisions. There is of course a lower limit, below which reduction of the time step does not lead to further accuracy [22].

Figure 5 shows the variation of D_s, calculated from MSD plots with $\delta t = 2$ fs, for three adsorbate densities at successive time intervals of 10,000 time-steps in the cylinder with radius 0.68 nm. At the lower reduced densities (2.67×10^{-5} and 2.28×10^{-4}) D_s exhibits quite large fluctuations and eventually drops to zero. At the highest density shown (1.3×10^{-3}), D_s shows no particular variation during the run, converging to its final value after about 30 intervals. It may be concluded that continuous increase of the total run time t, in order to obtain a precise D_s value, is not always applicable under the conditions where intermolecular collisions between moving molecules are highly infrequent. In the cylindrical geometry of the present investigation, molecules are subjected to high accelerations normal to the wall (the direction in which the potential field acts), but are not subject to any potential field parallel to the wall (along the z-axis). Rounding errors in the solution to the equations of motion therefore tend to distribute unequally between the degrees of freedom in these different directions under the influence of the thermostat, and the molecules eventually oscillate in the $x-y$ plane with little or no movement in the axial direction. A possible

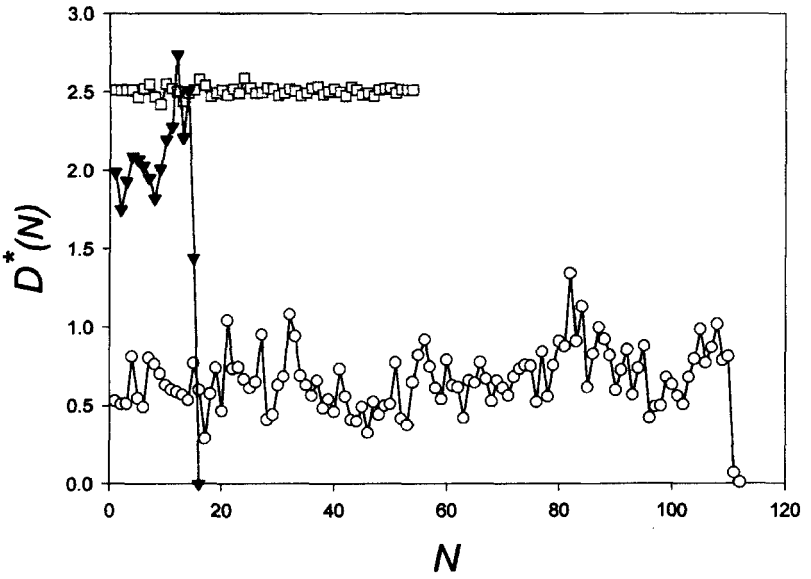

FIGURE 5 Reduced diffusion coefficient D_s^* as a function of the number N of successive time intervals of 10,000 time-steps and $\delta t = 2$ fs for CH_4 in the cylinder with $R = 0.68$ nm, for densities $\rho^* = 2.67 \cdot 10^{-5}$ (circles); $\rho^* = 2.28 \cdot 10^{-4}$ (triangles); and $\rho^* = 1.30 \cdot 10^{-3}$ (squares).

problem under conditions of strong localisation of the adsorbance molecules in model porous systems, is that high δt values lead to an increase in the ballistic part of the MSD curve since intermediate trajectories that could help randomisation are absent. Calculation of D_s by integrating the velocity autocorrelation function failed at the lowest density because of the significant noise in the long time tail and are therefore not reported in Tables I and II. Figure 6 illustrates the VACF for $R = 0.68$ and $\rho^* = 2.24 \times 10^{-4}$ with a time step of 1 fs.

3.2. Density Dependence of D_s

The self diffusion coefficients have been calculated at the densities shown in Tables I and II. A set of calculations was performed with $\varepsilon_{ss}/k = 395\,\text{K}$ as described above and a second set with $\varepsilon_{ss}/k = 650\,\text{K}$ corresponding to a much stronger adsorbing surface, with a holding potential similar to graphite. The density range is mainly within the Henry law region (up to $\rho^* \sim 0.02$). D_s was calculated from both the MSD and the VACF (except at the lowest density as explained above) and the two values were found to be in a satisfactory agreement.

Figure 7 shows the diffusivity as a function of density over the range of densities $10^{-5} - 10^{-3}$ for both cylinder radii and for both adsorbent surfaces.

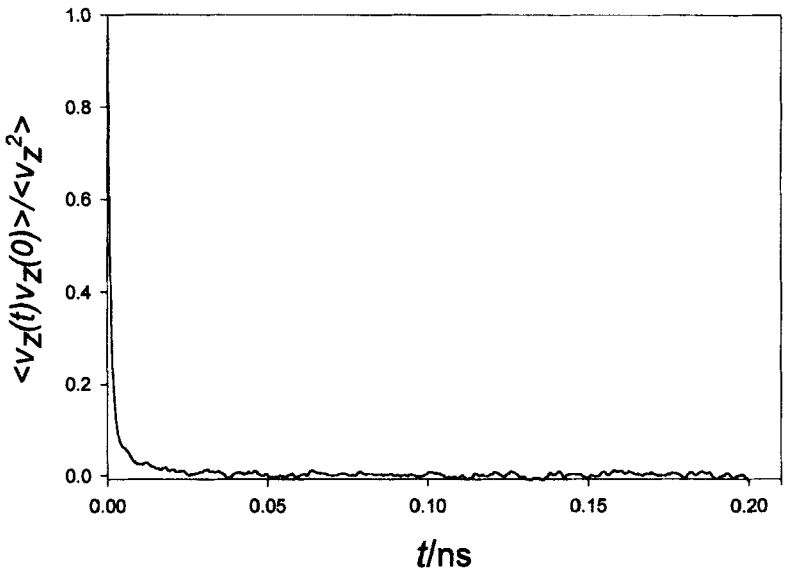

FIGURE 6 Normalised velocity autocorrelation plot along the direction of the flow, (z-axis), for $R = 0.68\,\text{nm}$ and $\rho^* = 2.28 \cdot 10^{-4}$ with $\delta t = 1\,\text{fs}$.

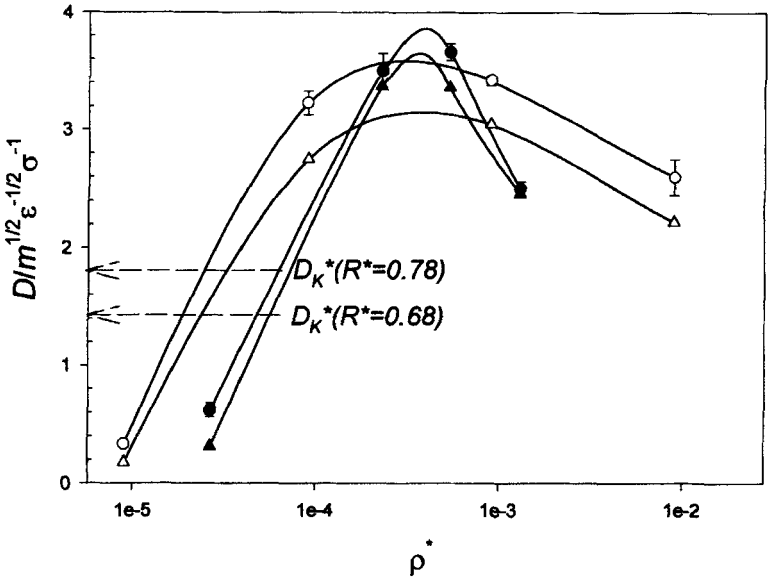

FIGURE 7 Reduced diffusion coefficient for methane in cylinders as a function of concentration (log scale) at 298 K. Filled symbols are for cylinders with radius 0.68 nm. Open symbols are for cylinders with radius of 0.78 nm. Circles denote a wall energy parameter, ε_{ss}/k_B = 395 K; triangles denote a wall energy parameter, ε_{ss}/k_B = 650 K.

The data have been averaged over all results for time steps of 1 and 2 fs and over results from MSD and VACF. The error bars are standard deviation from the mean of these values. The most notable observation is that D_s increases above the Knudsen value for both sizes of pore. High diffusivities in the Henry law region, have been previously observed [12–14] as discussed in the introduction. The present study confirms the occurrence of this phenomenon for cylindrical geometry and for adsorbate loadings well inside the Henry law region. In both pore sizes, the more strongly adsorbing surface (ε_{ss}/k = 650 K, shown as triangles) gives lower diffusion coefficients than the weakly adsorbing surface (ε_{ss}/k = 395 K, shown as circular points). The effect of changing the field appears to be greater for the larger pore. This is to be expected since most trajectories are small hops in which the molecules tend to vibrate normal to the surface. In the smaller pore, overlap effects produce a deeper potential in the centre of the cylinder (see Fig. 1) the mean vibrational amplitude normal to the surface is therefore greater, and longer hops are possible. It is also notable that the maximum is sharper for the smaller pore size (filled points).

The maximum in Figure 7 can be attributed to dynamic effects. In Figure 8, we show the mean separation distance between a pair of molecules

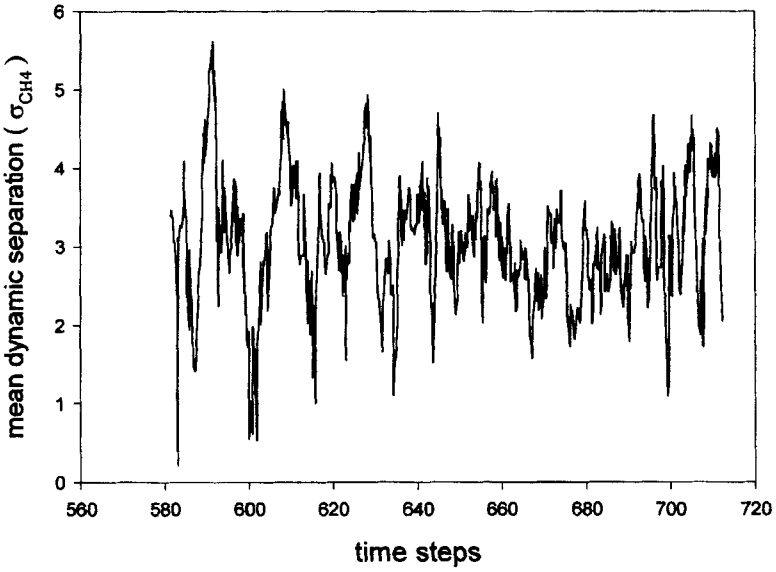

FIGURE 8 Magnitude of the mean separation vector between molecules in a cylinder with $R = 0.68$ nm at density of $\rho^* = 2.28 \cdot 10^{-4}$.

in the capillary of radius of 0.68 nm at a density 2.28×10^{-4} ($\varepsilon_{ss}/k = 395$ K) where the diffusivity is close to its maximum. Figure 8 shows that the mean separation oscillates around the value of $3\sigma_{gg}$, but with minima smaller than the hard sphere separation. Thus although the average intermolecular interactions are negligible at the low concentrations – as indicated by the linear Henry law plots – instantaneous dynamic interaction between molecules may occur.

Figure 9 shows a trajectory plot, for one particle in the above simulation, projected onto the $x-y$ plane. The full lines in Figure 9a correspond to the first 10900 time steps, and the circle is an envelope drawn around the maximum radial distance at which the trajectories are reversed. The arrow denotes the time step at which an intermolecular collision has occurred, resulting in a sharp reversal of the trajectory back towards the wall. The trajectory is shown in detail, for the time steps around this region, as the broken line in a magnified section in Figure 9b. It can be seen that the trajectory now penetrates deeply into the repulsive region of the wall and is therefore strongly accelerated away from the wall. The broken lines in Figure 9a follow the first few thousand time steps after this event. The longer time consequences are illustrated in Figures 9c and 9d, which show the next 3000 time steps, and the final 5000 time steps respectively. It can be

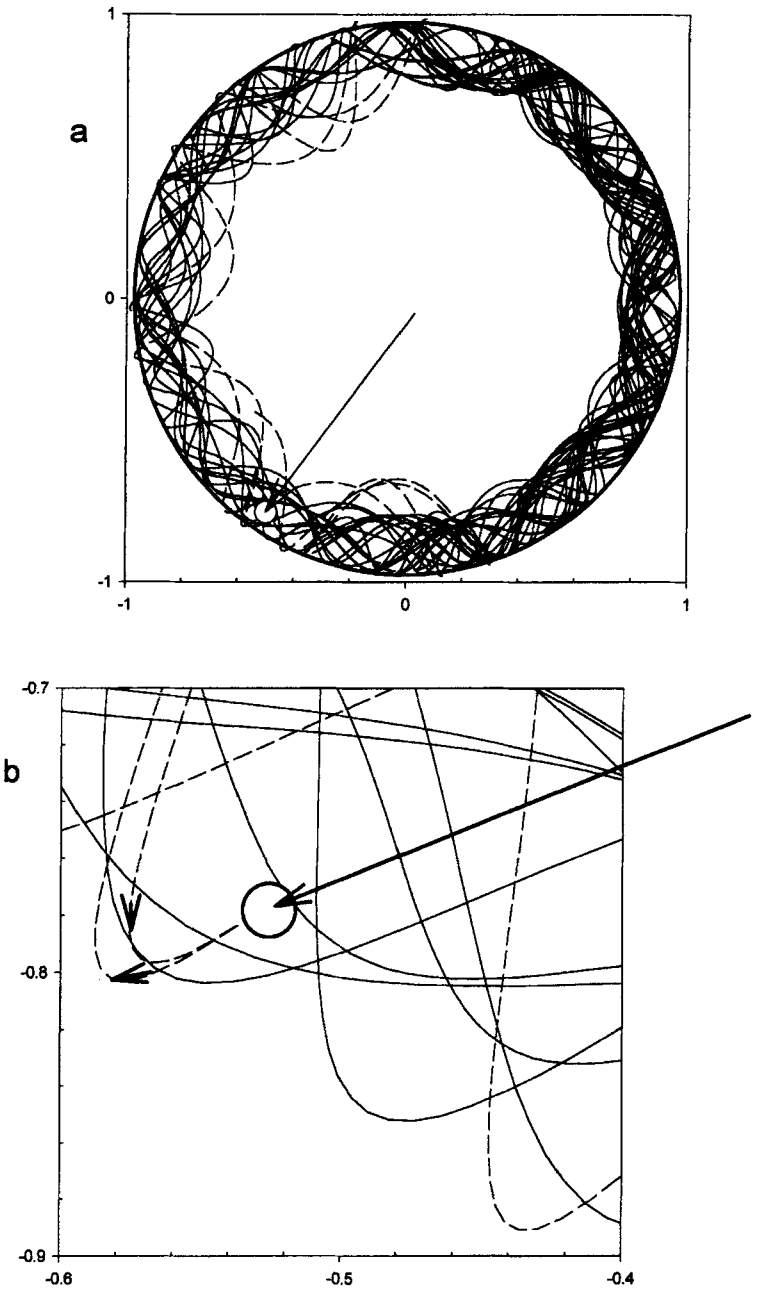

FIGURE 9 Trajectories of one molecule projected onto the cross-section (x, y plane) for a cylinder of physical radius $R = 0.68$ nm, at $\rho^* = 2.28 \cdot 10^{-4}$. (a) First 10900 time steps. (b) Detail from (a): see text. (c) time steps from 11000 to 15000. (d) Final 5000 time steps to 20000.

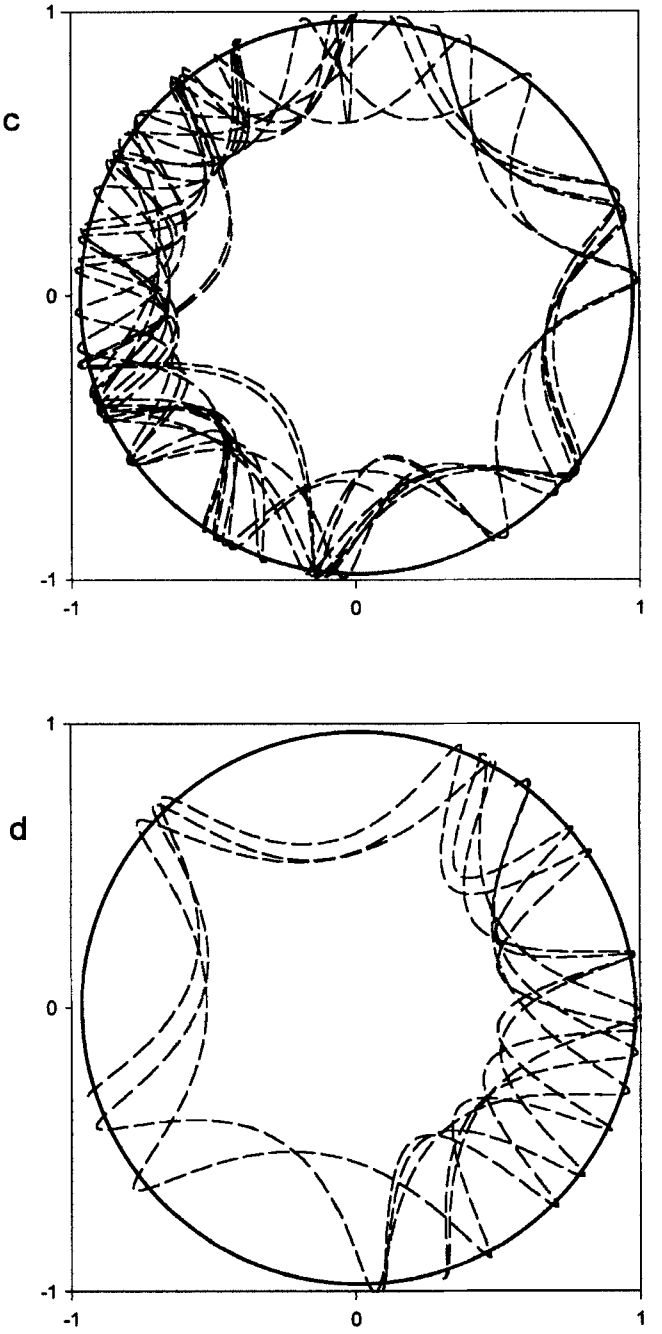

FIGURE 9 (Continued).

seen that much longer paths are occurring, and that the trajectory invariably penetrates the repulsive region of the wall potential. At the lowest concentration studied there is no evidence of this type of phenomenon. Figure 10 compares the mean free path distribution for the above run, with that for the run at the lowest density. The average value of the mean free path, $\langle \lambda \rangle$, from the distribution for the higher density run is 0.78σ which is much smaller than value for the cylinder of $4R_K^*/3 = 1.24\sigma$. The reduced mean speed is 2.3 at this temperature, giving a value for the reduced diffusion coefficient below 1.0, well below the estimated Knudsen value and the value of 3–4 found from the simulations. Clearly the high value of D_s^* cannot be explained in terms of a mean free path diffusion model. On the other hand, if we assume a hopping model, we can estimate the vibration frequency of molecules close to the wall using the second derivative of the potential energy at its minimum for the force constant. This gives a reduced frequency $\nu^* \sim 8.5$, and D_s^* from $\nu^* \langle \lambda \rangle^2/2$ is ~ 3.0 in satisfactory agreement with simulation. We may conclude that the hopping model, rather than the Knudsen model, is the more suitable description for diffusion of methane in micropores at ambient temperature.

At sufficiently low density, either intermolecular collision is such an improbable event that it does not occur over the whole length of the

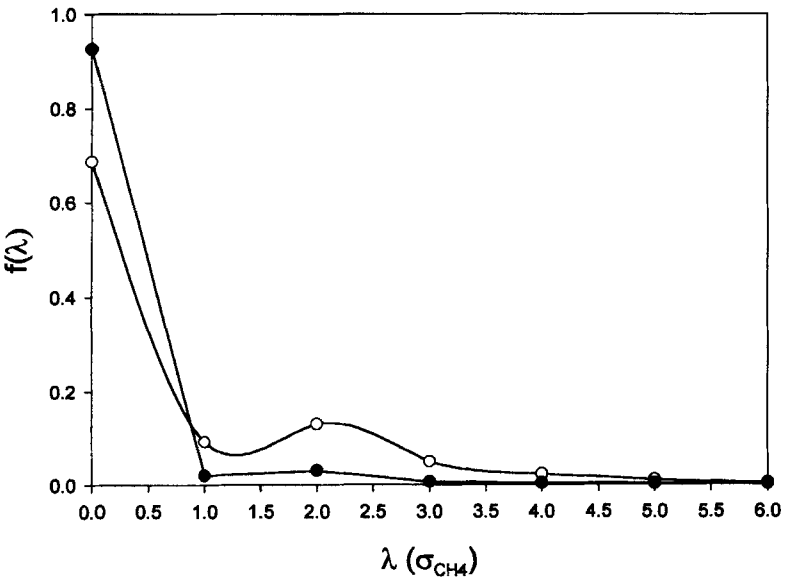

FIGURE 10 Mean free path histogram for the model of $R = 0.68$ nm and for the densities of $\rho^* = 2.67 \cdot 10^{-5}$ (filled circles) and $\rho^* = 2.28 \cdot 10^{-4}$ (open circles).

simulation, or else no collision occurs of the type illustrated in Figure 9. At higher densities, on the other hand, frequent intermolecular collisions serve to quench the longer trajectories revealed above, and diffusivity begins to decrease as a consequence.

4. DISCUSSION AND CONCLUSIONS

We have demonstrated that, with suitably short time steps and sufficiently long simulations, it is possible to obtain diffusion coefficients at low densities that are reproducible within acceptable error limits, for a Lennard-Jones molecule in confined spaces at ambient temperature. The degree of confinement is typical of that found in zeolitic and other microporous materials. Our simulation results show that at densities well within the Henry law region, diffusivity passes through a maximum with density that is well above the theoretical Knudsen value, whilst the limiting diffusivity is below this value. This maximum can be interpreted as being due to an infrequent collision event which causes a molecule to penetrate deeply into the repulsive region of the wall leading to long paths between wall collisions. In previous work [14] we have suggested that attractive interaction between molecules may produce a similar phenomenon, but no evidence of this type of effect was found here. Earlier suggestions that similar diffusion maxima may be due to molecules being freed from deep potential pockets do not apply in the system studied in this work. The diffusion mechanism in this system is more consistent with a hopping model than with the classical Knudsen mechanism.

A question that needs to be asked is whether diffusion maxima at low density are in fact artefacts of simulation studies without correlates in the real world. One problem is that the phenomenon is related to rare events, and total simulation times (even in very long runs) are extremely short on the time scale of most experiments. However this objection does not rule out the possibility that such phenomena could occur at even lower concentration. A second difficulty is the inherent inaccuracy of the numerical solution of the equations of motion. We have seen that this can eventually cause the axial diffusion to collapse to zero. It seems improbable that this defect could also be responsible for the opposite effect. In this work we have used the Verlet algorithm, and it is possible that alternative algorithms may lead to slower accumulation of rounding errors [22], however it is not clear that this would eliminate the phenomenon under discussion. A further point is that the proffered explanation is crucially dependent on the way in which all

molecular velocities are randomised, in accordance with the cosine reflection law [23]. Another possibility is to model the wall atoms as if they were localised vibrators. Objections can be raised against all these models. However it is arguable that the mechanism observed here would occur in real systems. The essential feature is that a rare intermolecular collision propels an adsorbate molecule deeply into the repulsive part of its interaction with a wall atom and that subsequent long trajectories are not quenched over a relatively long period of time.

Acknowledgements

We would like to thank the CEC (grant JOULE: JOE3 – CT95-0018) the EPSRC (grants GR/K83878 and GR/L80812) and KOSEF for support.

References

[1] Steele, W. A., In: *Transport Phenomena in Fluids*, Ed. Hanley, H. J. M., Marcel Dekker, New York, 1969, pp. 209–264.
[2] Hansen, J. P. and McDonald, I. R., *Theory of Simple Liquids*, Academic Press, London, 1986.
[3] Karger, J. and Ruthven, D., *Diffusion in Zeolites and Other Micropores Solids*, Wiley, New York, 1992.
[4] Theodorou, D. N., Snurr, R. Q. and Bell, A. T., In: *Comprehensive Supramolecular Chemistry*, Vol. 7, Eds. Alberti, G. and Bein, T., Pergamon, New York, 1997, pp. 507–548.
[5] Magda, J. J., Tirrell, M. and Davis, H. T. (1985). "Molecular dynamics of narrow liquid filled pores", *J. Chem. Phys.*, **83**, 1888.
[6] MacElroy, D. M. and Suh, S.-H. (1987). "Computer simulation of moderately dense hard-sphere fluids and mixtures in microcapillaries", *Mol. Phys.*, **60**, 475.
[7] June, R. L., Bell, A. T. and Theodorou, D. N. (1990). "Molecular dynamics study of methane and xenon in silicalite", *J. Phys. Chem.*, **94**, 8232.
[8] Demi, T. and Nicholson, D. (1991). "Molecular dynamics simulation studies of the density and temperature dependence of self-diffusion in a cylindrical micropore", *Molecular Simulation*, **5**, 363.
[9] Maginn, E. J., Bell, A. T. and Theodorou, D. N. (1993). "Transport diffusivity of methane in silicalite from equilibrium and nonequilibrium simulations", *J. Phys. Chem.*, **97**, 4173.
[10] Cracknell, R. F. and Gubbins, K. E. (1993). "Molecular simulation of adsorption and diffusion in VPI-5 and other aluminophosphates", *Langmuir*, **9**, 824.
[11] Cracknell, R. F., Nicholson, D. and Quirke, N. (1995). "Direct molecular simulation of flow down a chemical potential gradient in a slit shaped pore", *Phys. Rev. Lett.*, **74**, 2463.
[12] Cracknell, R. F., Nicholson, D. and Gubbins, K. E. (1995). "Molecular dynamics study of the self-diffusion of supercritical methane in slit-shaped graphitic micropores", *J. Chem. Soc. Faraday Trans.*, **91**, 1377.
[13] Nicholson, D. and Cracknell, R. F. (1996). "Self diffusion and transport in slit shaped pores", *Fundamentals of Adsorption V*, Kluwer Academic Publishers, 683.
[14] Nicholson, D. (1998). "Simulation studies of methane transport in model graphitic micropores", *Carbon*, **10**, 1511.
[15] Nicholson, D. and Petropoulos, J. H. (1981). "Calculation of the surface flow of a dilute gas in model pores from first principles", *J. Colloid Interface Sci.*, **83**, 420.

[16] Levitz, P. (1997). "From Knudsen diffusion to Levy walks", *Europhys. Lett.*, **39**, 593.
[17] Chitra, R. and Yashonath, S. (1997). "Estimation of error in the diffusion coefficient from molecular dynamics simulations", *J. Phys. Chem. B*, **101**, 5437.
[18] Nicholson, D. and Gubbins, K. E. (1996). "Separation of dioxide-methane mixtures by adsorption: Effects of geometry and energetics on selectivity", *J. Chem. Phys.*, **104**, 8126.
[19] Davis, M. E. *et al.* (1989). "Physicochemical properties of VPI-5", *J. Am. Chem. Soc.*, **111**, 3919.
[20] Kiselev, A. V., Lopatkin, A. A. and Shulga, A. A. (1985). "Molecular statistical calculation of gas adsorption by silicalite", *Zeolites*, **5**, 261.
[21] Allen, M. P. and Tildesley, D. J., *Computer Simulation of Liquids*, Oxford University Press, Oxford, 1987.
[22] Haile, J. M., *Molecular Dynamics Simulation: Elementary Methods*, Wiley, New York, 1992.
[23] Valleau, J. P., Diestler, D. J., Cushman, J. H., Schoen, M., Hertzner, A. W. and Riley, M. E. (1991). "Comment on: Adsorption and diffusion at rough surfaces. A comparison of statistical mechanics, molecular dynamics and kinetic theory", *J. Chem. Phys.*, **95**, 6194.